# Laser written nanoporous silicon diffraction gratings for biosensors

**Jinan Xia,[1, 2] Andrea. M. Giovannozzi [2], Sheila. J. Sadeghi[3], Ginafranco Gilardi[3], and Andrea M. Rossi[2,*]**

[1]*Materials and Microsystems Laboratory, Department of Applied Science and Technology, Politecnico di Torino, corso Duca degli Abruzzi, 24, 10129 Torino, Italy*
[2] *Nazionale di Ricerca Metrologica, Strada delle Cacce, 91, 10135 Torino, Italy*
[3]*Centre of Excellence in Nanostructured Interfaces and Surfaces - Department of Human and Animal Biology, University of Torino, Via Accademia Albertina, 13, 10123, Torino, Italy*
**Corresponding author: a.rossi@inrim.it*

Received Month X, XXXX; revised Month X, XXXX; accepted Month X, XXXX;
posted Month X, XXXX (Doc. ID XXXXX); published Month X, XXXX

Surface-relief diffraction gratings and planar diffraction gratings directly written on nanoporous silicon layers using 514 nm continuous wave lasers at very low power (less than 20 mW) were demonstrated. Diffraction-based biosensing application to detect arachidonic acid was experimentally demonstrated at incident light wavelength of 632.8 nm. Laser written gratings enable directly immobilizing bio-molecules in the laser oxidized area of nanoporous silicon, resulting in a new patterned functionalization technique for biosensing applications. The functionalization technique can not only simplify the functionalization procedure in biosensing but also it has potential to increase the sensitivity of sensors by accurately defining grating patterns using the laser direct writing technique.
*OCIS codes:* （280.1415） Biological sensing and sensors; (050.1950) Diffraction gratings; (160.4236) Nanomaterials；（240.3990） Micro-optical devices.
http://dx.doi/org/10.1364/AO.99.099999

## 1. Introduction

Optical diffraction gratings based on different materials have found numerous applications in biosensing field. Biochemical species are selectively bound onto the top surface of a diffraction grating leading to changes in the effective depth of the grating, and in the refractive index contrast [1-3]. These variations can be detected by measuring light diffraction intensities. Tantalum pentoxide diffraction grating sensors were reported to study dynamic response of antibody interaction with protein G adsorbed on the sensing surface [4]. Hydrogel grating was used to detect the glucose concentration [5]. Gold and silver gratings based on surface plasmon resonance were reported for high sensitivity sensors [6, 7] and grating waveguide couplers were reported for biosensors as well [8]. However, similar to other traditional biosensors, limited surface areas on the gratings are available for biochemical attachments, ultimately limiting the sensitivities of the sensors. Measurement often requires signal amplification in order to achieve satisfactory sensitivities [9, 10]. Nanoporous silicon has attracted interest in chemical and biological sensing due to its favorable properties [11, 12]. It provides large internal surface area and tunable porosity, and it can be easily formed in silicon wafer with low cost and simple fabrication technique. Large internal surface area enables more effective capture and detection of chemical and biological molecules in sensing applications, and it can drastically increase sensor sensitivity.

Most of the cited gratings are fabricated by photolithography that usually requires long time preparation procedure and expensive instrumentation. Laser direct-writing has been applied to fabricate optical gratings. Many reports show that femtosecond pulsed lasers are used for the fabrication [13], since they provide high peak power in a short time and yield very small heat affecting zone during laser interacting with the processed materials. But, femtosecond lasers are expensive and they need complicated operation maintenance. Low power lasers were also reported to be used to write submicron structures at glass surface [14]. For biosensing purpose, here we demonstrate diffraction gratings directly written on nanoporous silicon layers fabricated using very low power laser. This is the first to report direct writing gratings on nanoporous silicon layers using very low laser power, to our knowledge. In particular, we report that surface functionalization for sensing purpose is achieved directly on laser writing lines in the fabricated porous silicon planar gratings, and that biomolecules are selectively bound to the laser oxidized area, which can not only simplify the functionalization procedure in biosensing but also increase the sensitivity of the sensors by accurately defining grating patterns using the laser direct writing technique. As proof of concept, we demonstrate sensing experiment to use the gratings for biosensors.

## 2. Fabrication of Surface-Relief Diffraction Gratings and Planar Diffraction Gratings

Porous silicon was prepared by electrochemical etching of <100> p++ crystal silicon wafers in a 37% hydrofluoric acid solution in ethanol. A current density of 100 mA/cm$^2$ was applied reaching a total PS thickness of 10 μm. Diffraction gratings were

fabricated by direct writing method using a 514 nm argon ion laser beam. The laser beam was focused by a 60× microscope objective on PS surface inducing a laser local thermal oxidation of silicon nanostructures. The PS sample is placed on a 2D motorized stage driven by a computer, any pattern can be in principle produced. The laser direct writing process is the same as that was reported for the fabrication of nanoporous silicon waveguides [15]. Gratings with periods ranging from 3 to 7 µm

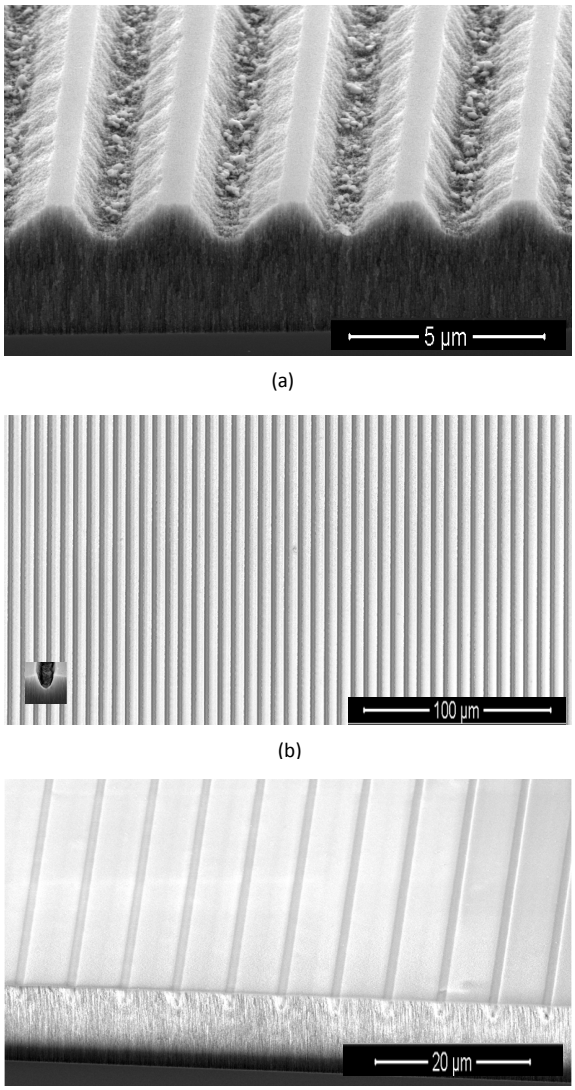


Fig. 1 (a) Scanning electron microscope (SEM) cross section of a relief grating with a period of 3 µm; (b) SEM top view of a relief grating with a grating period of 7 µm; (c) SEM top view of PS planar grating showing a grating period of 7 µm. All the grating depths are close to 2 µm.

were fabricated by using a continuous wave argon ion laser at the power up to 20 mW and a laser scanning speed up to 400 µm/s. Two types of gratings i.e. relief gratings and planar gratings were fabricated in our work as shown in Fig. 1. For the relief gratings shown in Fig. 1(a) and (b), samples were immersed into dilute HF solution after writing procedure to remove the porous silicon oxide lines produced by laser beam. Figure 1(a) shows the scanning electron microscope (SEM) cross section of a relief grating with a period of 3 µm. Figure 1(b) shows the top view of a relief grating with a period of 7 µm. The insert shows the magnified cross section of one trench of the grating. Figure 1(c) shows SEM cross section of a planar grating with a period of 7 µm and PS oxide lines are not removed after laser beam irradiation. Depth and pitch are the same measured in the relief grating. All the gratings have almost the same depth close to 2 µm. The porous silicon layers have also the same porosities and the refractive indices for both the relief gratings and planar grating. Pore size distribution was measured to be around 50 nm in diameter. All the porous silicon layers have the porosities of around 65% with a refractive indies of around 1.7781-0.0034i at the wavelength of 632.8 nm. The refractive indices and porosities of the porous silicon layers were obtained by fitting reflection spectral of single corresponding layers.

## 3. Surface Functionalization of Gratings for Biosensors

Both types of gratings were bioconjugated with the heam domain (BMP) of the Cytochrome P450 BM3 (CYP102A1) from Bacillus megaterium. A BMP cysteine mutant was labeled with the fluorescent probe IANBD (absorption $\lambda_{max}$ 478 nm, emission $\lambda_{max}$ 540 nm) and used to selectively bind the arachidonic acid (AA) which is a well known biomarker involved in pain and inflammation processes [16], and also in a number of diseases such as Alzheimer's [17], liver cancer [18, 19] and kidney pathologies [20]. This biorecognition system was used to demonstrate, as proof of concept, the biosensor configuration of these gratings. For biomolecules immobilization protocol a silicon oxide surface is required and therefore two different functionalization chemistries were used for relief and

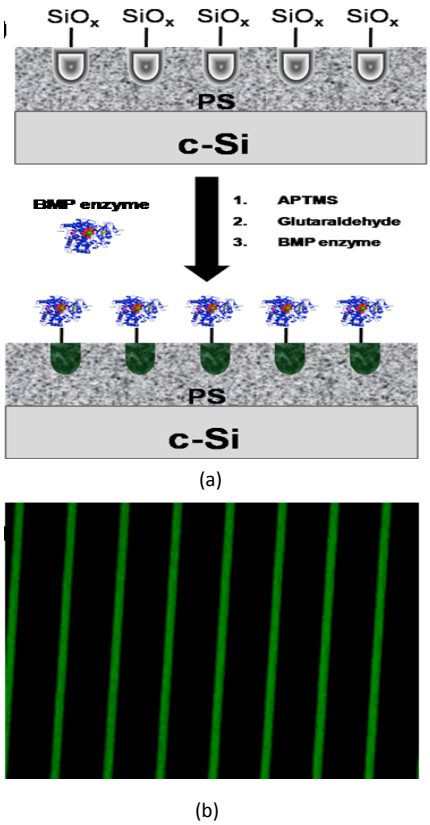


Fig. 2 (a) Patterned functionalization chemistry used for the planar grating in order to selectively attach the BMP enzyme into the oxide regions; (b) Fluorescence image of planar grating surface.

planar gratings. A summary of the functionalization steps are shown in Fig. 2(a) and Fig. 3(a) respectively. For the planar grating, a patterned immobilization of the biomolecule was developed. This new patterned functionalization technique was achieved by exploiting the different chemistry of the as-etched PS regions (Si-Hx terminated) and the adjacent laser written oxidized lines (Si-Ox terminated). Since the silanization reaction with APTMS only occurs at the silicon oxide regions, the BMP enzyme was selectively bound to the oxidized lines. Samples were then cured in oven to stabilize the PS surface that was afterwards modified with gluteraldehyde and BMP enzyme. Fluorescence image of the planar grating (Fig. 2(b)) clearly demonstrates the selective attachment of the BMP only on the oxide lines. For the relief grating, the relief grating was oxidized in oven at 500 °C for 3 hours, silanized with a 5% 3-aminopropyltrimethoxysilane (APTMS) ethanol solution, then treated with a 2.5% glutaraldehyde aqueous solution and incubated with 10 μM BMP enzyme in sodium phosphate buffer (pH 7.4). Details of chemistry and procedures were reported elsewhere[21]. Fluorescence image of the relief grating (Fig. 3(b)) shows the BMP distribution on the entire surface of the device. While the relief grating was completely grafted with the BMP enzyme.

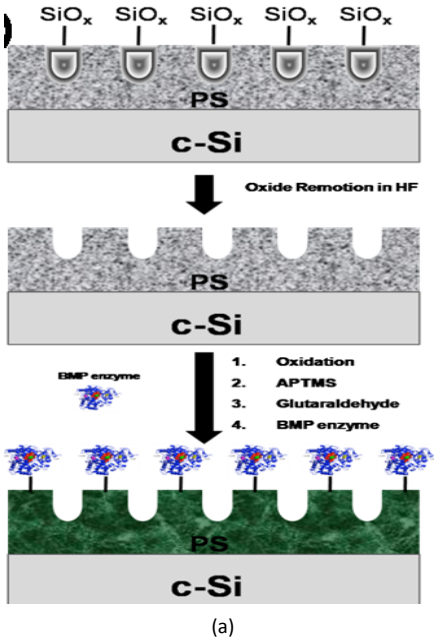


(a)

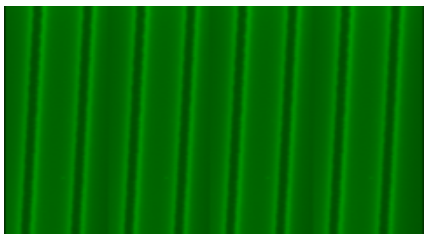

(b)

Fig. 3 (a) Functionalization chemistry used for the relief grating: in order to attach the BMP enzyme; (b) Fluorescence image of relief grating surface.

## 4. Biosensing experiment and discussion

Sensing experiments were performed using a single diagnostic concentration of arachidonic acid (AA, 200 μM) that was observed in some pathological conditions such as liver cancer and psoriasis. A schematic of the experimental setup using the gratings for biosensing analysis is shown in Fig. 4. A He-Ne laser at the wavelength of 632.8 nm was used as the light source. Light from the laser was attenuated by an adjustable filter and was incident on the surfaces of the gratings. The gratings have periods of 4 μm and their footprints on the porous silicon layers are 1.5 mm wide and 2 mm long. Light diffraction patterns of the gratings were imaged on a CCD camera.

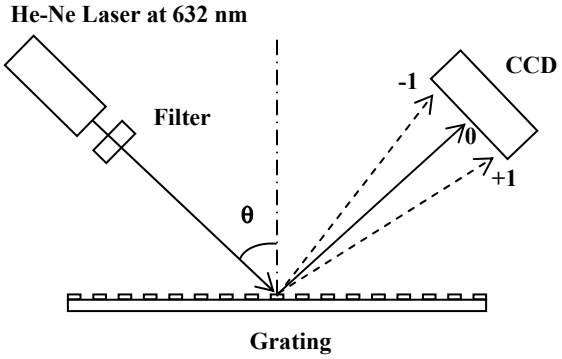


Fig. 4. Schematic of experimental setup used for biosensing analysis.

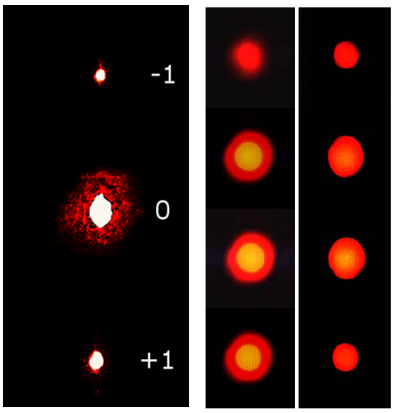


Fig. 5. Left: Camera images of light diffraction patterns for diffraction orders m= -1, 0, +1. Right: The first order m = 1 diffraction light patterns for planar gratings (left column) and relief gratings (right column). From top to bottom, the images are the diffraction patterns from the fresh grating and the grating functionalized with APTMS, BMP, and AA respectively.

The diffraction patterns at different diffraction orders are shown in Fig. 5. On the left side of Fig. 5, the camera images of light diffraction patterns for diffraction orders m= -1, 0, +1 are shown. Both the first order ($m_1$ and $m_{-1}$) relative diffraction intensities and diffraction pattern positions on the CCD can be used for transduction in arachidonic acid sensing. Light diffraction intensities of the gratings change after surface functionalization and subsequently after molecule immobilization into the gratings. Changes of light diffraction intensities and their pattern positions depend on the refractive index variation, fill factor change of porous matrix, and grating period change caused by molecule immobilization as well as light incident angles. When grating period and light incident

angle are fixed, the light diffraction intensities will change with the refractive index of the gratings. As can been seen on the right side of Fig. 5, the images in the left column report the change of the first order (m = 1) diffraction light patterns and intensities for planar grating, and the images in the right column reports the change of the first order (m = 1) diffraction light patterns and intensities for relief grating. In the two columns, from top to bottom they are the diffraction patterns of the fresh grating, the grating which was treated with APTMS, the grating which was applied with BMP, and the grating which was functioned with AA. Light diffraction intensities increase in the first two steps, i.e., in the steps of surface functionalization and subsequent molecule immobilization. The light diffraction intensities decrease in the last step, i.e. in the step of functionalization with AA. Actually, the changes in the first order (m = 1) light diffraction intensities in the last step are used for transduction in our arachidonic acid sensing, because they can directly detect the changes in sensed biological molecule concentrations or molecule numbers. Meanwhile, changes in the diffraction pattern positions on the CCD can be evaluated for associate transduction in the arachidonic acid detection.

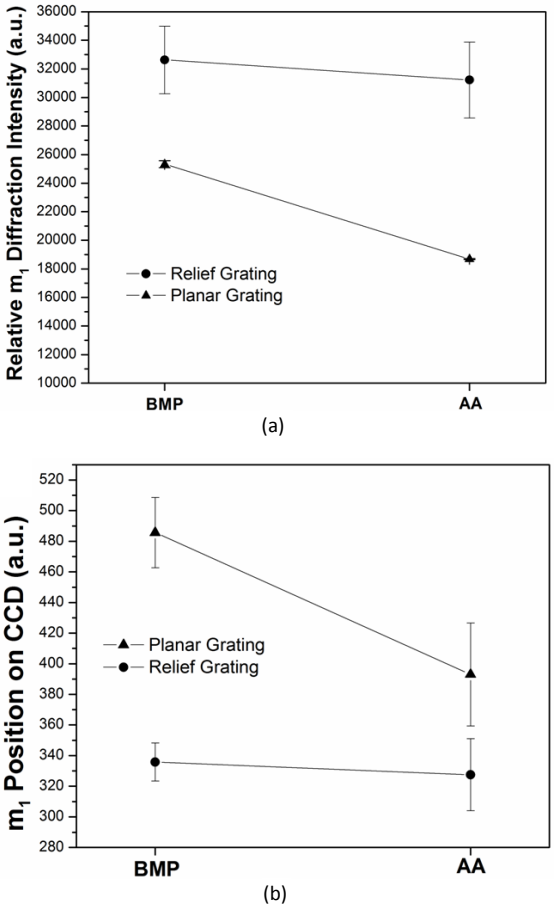


Fig. 6. (a) Change of the first order diffraction intensity on CCD camera for relief (circle) and planar (triangle) gratings before and after incubation with AA; (b) Change of the first order diffraction pattern position on CCD camera for relief (circle) and planar (triangle) grating before and after incubation with AA before and after incubation with AA.

The typical experimental results in both intensity and position changes at the last step are shown in Fig. 6. The light diffraction intensity and the pattern position of the diffracted light were calculated by using ImageJ software. Sensing measurements were performed before and after the grating exposure to the arachidonic acid. As shown in Fig. 6(a), after the incubation with the arachidonic acid, a change of the $m_1$ order light diffraction intensity is clearly seen for the planar grating. A slightly decrease could be also seen in the relief grating. Higher sensitivity of the planar grating than the relief one can be further seen by checking the position change of the $m_1$ spot on the CCD. The shift of the $m_1$ order spot position is caused by a change of the light diffraction angle that is related to a change of the refractive index inside the grating. While slight change was seen in the relief grating, a significant shift was seen in the planar grating after the arachidonic acid exposure (Fig. 6(b)). An explanation of the different behaviors of the two gratings relies on the different bioconjugation processes used. Since the AA-BMP binding occurs on the entire relief grating, the change of the refractive index contrast between the porous silicon and air void in relief grating is not sensitive enough to promote a significant change in light diffraction efficiency and spot position. In the planar grating, instead, since the AA is selective captured by the BMP enzyme into a pattern, the change of refractive index contrast between two adjacent areas of porous silicon is higher enough to promote a change in both intensity and position of the first diffraction order. Negative control solutions using the sole phosphate buffer were also employed (not shown) and they demonstrated to not perturb both $m_1$ diffraction order intensity and position in the planar grating. These collected changes were then related only to the presence of the arachidonic acid.

## 5. Conclusion

Surface-relief diffraction gratings and planar diffraction gratings directly written on nanoporous silicon layers using 514 nm continuous wave lasers at low power (less than 20 mW) were demonstrated. Directly immobilizing bio-molecules in the laser oxidized area of the nanoporous silicon gratings were realized. This provides a simple and easy–patterned functionalization technique for biosensing applications. The functionalization technique can not only simplify the functionalization procedure in biosensing but also it has potential to increase the sensitivities of sensors by accurately defining grating patterns using the laser direct writing technique. Diffraction-based biosensing application to detect arachidonic acid was experimentally demonstrated at incident light wavelength of 632.8 nm, indicating that the low power laser written gratings have potential to be used for high quality and high sensitivity biosensors. The grating periods can be further reduced to sub-micrometers by using higher magnification microscope objectives to reduce the spot of the focused laser beam on the processed samples [14], or by increasing the scanning speed of the laser beam. Using the gratings with small periods can further increase the sensitivities of the grating-based sensors.

For the writing of relief gratings and planar gratings on the nanoporous silicon layers, the laser can be replaced by many other lasers at visible wavelengths. It will drastically reduce cost

in grating fabrication. The demonstration of the bio-sensing experiment based on the laser written gratings shows that very low power laser direct-writing can provide easy and highly efficient approach to fabricate high quality gratings on nanoporous silicon layers for biosensing applications.

## References


1. R. Jenison, S. Yang, A. Haeberli, and B. Polisky, "Interference-based detection of nucleic acid targets on optically coated silicon," Nat. Biotechnol. **19**, 62-65 (2001).

2. J. B. Goh, R. W. Loo, and M. C. Goh, "Label-free monitoring of multiple biomolecular binding interactions in real-time with diffraction-based sensing," Sens. Actuators **B106**, 243-248(2005).

3. C. Chang, G. Acharya, C. A. Savran, "*In situ* assembled diffraction grating for biomolecular detection," Appl. Phys. Lett. **90**, 233901 (2007).

4. R. Polzius, Th. Schneider, F.F. Biert & U. Bilitewskit, "Optimization of biosensing using grating couplers: immobilization on tantalum oxide waveguides," Biosens. and Bioelectr. **11**, 503-514(1996).

5. G. Ye, X. Wang, "Glucose sensing through diffraction grating of hydrogel bearing phenylboronic acid groups," Biosens. and Bioelectr. **26**, 772-777 (2010).

6. J. Dostalek, J. Homola, M. Miler, "Surface plasmon resonance sensor based on an array of diffraction gratings for highly parallelized observation of biomolecular interactions," Sensors and Actuators **B 129**, 303-310 (2008).

7. J. Homola, S. S. Yee, G. Gauglitz, "Surface plasmon resonance sensors: review," Sensors and Actuators **B 54**, 3-15 (1999).

8. J. Vörös, J. J. Ramsden, G. Csúcs, I. Szendro, S. M. De Paul, M. Textor, N. D. Spencer, "Optical grating coupler biosensors," Biomaterials. 2**3**, 3699-3710 (2002).

9. J. Lee, K. Icoz, A. Roberts, A. D. Ellington, and C. A. Savran, "Diffractometric Detection of Proteins Using Microbead-Based Rolling Circle Amplification,"Anal. Chem. **82**, 197-202 (2010).

10. A. W. Wark, H. J. Lee, A. J. Qavi, and R. M. Corn, Anal. Chem. **79**, 6697 (2007).

11. L. Canham, *Properties of Porous Silicon* (INSPEC, London, 1997).

12. V.S.Y. Lin, K. Motesharei, K.P.S. Dancil, M.J. Sailor, M.R. Ghadiri, "A porous silicon-based optical interferometric biosensor," Science **278**, 840-843 (1997).

13. R. Mart´ınez-Vazquez, R. Osellame, G. Cerullo, R. Ramponi, and O. Svelto, "Fabrication of photonic devices in nanostructured glasses by femtosecond laser pulses," Opt. Express 15, 12628-12635 (2007).

14. M. Thie, J. Fischer, G. von Freymann, and M. Wegener, "Direct laser writing of three-dimensional submicron structures using a continuous-wave laser at 532 nm,"Appl. Phys. Lett. **97**, 221102 (2010).

15. A. M. Rossi, G. Amato, V. Camarchia, L. Boarino, and S. Borini, "High-quality porous-silicon buried waveguides,"Appl. Phys. Lett. **78**, 3003 (2001).

16. D. Panigrahy, A. Kaipainen, E. R.Greene, S. Huang, "Cytochrome P450-derived eicosanoids: the neglected pathway in cancer,"Cancer Metast. Rev. **29** , 723 -735(2010).

17.R.O. Sanchez-Mejia, L. Mucke, "Phospholipase A2 and arachidonic acid in Alzheimer's disease," Biochim. Biophys. Acta **1801**, 784-790 (2010).

18.D. Dymkowska, J. Szczepanowska, M. R.Wieckowski, L. Wojtczak, "Short-term and long-term effects of fatty acids in rat hepatoma AS-30D cells: The way to apoptosis," Biochim. Biophys. Acta **1763**, 152 -163 (2006).

19. Z.G. Xu, M. Zhang, X.Y. Lv, D. Xiang, X. Zhang, L. Chen, Biochem. "The inhibitory effect of celecoxib on mouse hepatoma H22 cell line on the arachidonic acid metabolic pathway," Cell Biol. **88**, 603-609 (2010).

20. P. Su, K. M. Kaushal, D. L. Kroetz, "Inhibition of renal arachidonic acid ω-hydroxylase activity with ABT reduces blood pressure in the SHR*,"*Am. J. Physiol. **275**, R426-R438 (1998).